DOE/JPL/956786-85/3
(DE85008302)
Distribution Category UC-63b

DEVELOPMENT OF HIGH-EFFICIENCY SOLAR CELLS ON SILICON WEB

A. Rohatgi, D. L. Meier, R. B. Campbell,
T. W. O'Keeffe, and P. Rai-Choudhury

Third Quarterly Progress Report
October to December 1984

This work was performed for the
Jet Propulsion Laboratory

Contract No. 956786

February 5, 1985

Westinghouse R&D Center
1310 Beulah Road
Pittsburgh, Pennsylvania 15235

TABLE OF CONTENTS

Blank Page

LIST OF FIGURES

Blank Page

LIST OF TABLES

Blank Page

1. SUMMARY

During this period emphasis was placed on the development of process techniques that will enhance web cell performance. We have: (a) established the oxidation conditions to passivate web cells to reduce surface recombination velocity, (b) developed evaporated double-layer antireflective coating using ZnSe and MgF_2 films to minimize reflection losses from the front surface, and (c) developed an aluminum back-surface reflector to utilize the unabsorbed long-wavelength photons.

We have also fabricated web solar cells by incorporating the above advanced features. Efficiencies as high as 16.9% were obtained on 1 cm × 1 cm dendritic web silicon cells on 0.37 ohm-cm web crystals. A combined effect of oxide passivation, evaporated double-layer AR coating, and back-surface reflector gave ~ 59% improvement in the short-circuit current and 69% increase in cell efficiency compared to the counterpart baseline cell with no passivation, AR coating, or back-surface reflector.

During this period we also grew low-resistivity web crystals (0.37 ohm-cm, crystal #4-275) to take the advantage of heavy doping in the base. It is important to realize that a low-resistivity, high-lifetime base is an ideal material for high-efficiency cells. Reasonable diffusion lengths (~ 150 μm) were obtained in the finished low-resistivity web cells, encouraging further investigation for achieving high efficiency in web cells.

2. INTRODUCTION

The idealized efficiency[1] of a silicon solar cell is about 25%, assuming the best material and surface parameters achievable to date, although present day cells fall considerably short of this limiting value. This is largely a consequence of heavy doping effects, bandgap narrowing, and high recombination at and near the cell surfaces. The major problems of efficiency improvement fall in the above categories; however, additional design requirements are essential for efficient contacts and antireflective coating. Although these areas are well understood, they are not insignificant and must be optimized consistent with device structure.

Starting material is equally important for high-efficiency cells because device fabrication and design are academic if the starting material quality is poor or it degrades rapidly with processing. The objective of this program is to understand and improve web silicon so that high-efficiency web cells can be fabricated using advanced cell design and processing.

It is clear that high efficiency is a major attribute that will enhance the large-scale applicability of photovoltaic systems. Systems calculations indicate that for very large-scale terrestrial applications, $\geq$ 15% efficient photovoltaic modules will be required at a cost of $\sim$ 50¢/watt. This implies that $\sim$ 18% efficient cells will be needed at low cost. Dendritic web silicon is a single-crystal silicon ribbon that has great potential for low-cost and high-efficiency solar cells. In this program we are trying to understand the loss mechanisms in dendritic web silicon by investigating the electrical activity of twin planes, the role of impurities and defects in web, impurity interaction with twin planes, starting web material quality, and the effect of heat

treatment and gettering on web quality. An improved understanding of the above effects should lead to fabrication of ~ 18% efficient web cells with good uniformity. This second quarterly report describes progress toward the development of high-efficiency solar cells on web silicon. We report here the development of evaporated double-layer AR coating and aluminum back-surface reflector. Also shown are results on 16.9% efficient web cells achieved on 0.37 ohm-cm web crystal by the combination of oxide passivation, double-layer AR coating, and aluminum back-surface reflector.

3. TECHNICAL PROGRESS

3.1 Double-Layer Antireflective Coating

3.1.1 Development of ZnSe + MgF_2 Double-Layer Antireflective Coating

We have attempted to develop an evaporated double-layer AR coating by using ZnSe and MgF_2 films, both of which are thermally evaporated. Evaporated ZnSe film showed a refractive index of 2.57 and MgF_2 an index of 1.38. Model calculations in Figure 1 show that 548 Å ZnSe + 1040 Å MgF_2 on top of the bare silicon surface can provide 51.7% enhancement in the short-circuit current density. However, if 100 Å passivating oxide is present, then the thicknesses have to be adjusted to 398 Å ZnSe and 1080 Å MgF_2 in order to get 51.7% improvement in J_{sc}.

The above calculations assume no absorption in the films. We have measured the absorption in the ZnSe film by measuring the reflectance (R) and the transmittance (T) of 475 Å ZnSe film deposited on a glass slide. Absorption (A) can be obtained by

$$A(\lambda) = 1-\{R(\lambda + T(\lambda)\}$$

Figure 2 shows the measured plots for R, T, and A. There is some absorption in the ZnSe film in the wavelength below 0.55 μm, and at about 0.4 μm it is as much as 20%. Above an 0.55 μm wavelength, there is no absorption at all.

Figure 3 shows the measured reflectivities of a) 475 Å ZnSe film, b) 1000 Å MgF_2 film on silicon, and c) 475 Å ZnSe + 1000 Å MgF_2 on a silicon surface.

Table 1 shows the results on actual solar cells. Both ZnSe and MgF_2 were deposited by thermal evaporation in one pump-down. These cells had no oxide passivation, so we evaporated 550 Å ZnSe + 1040 Å

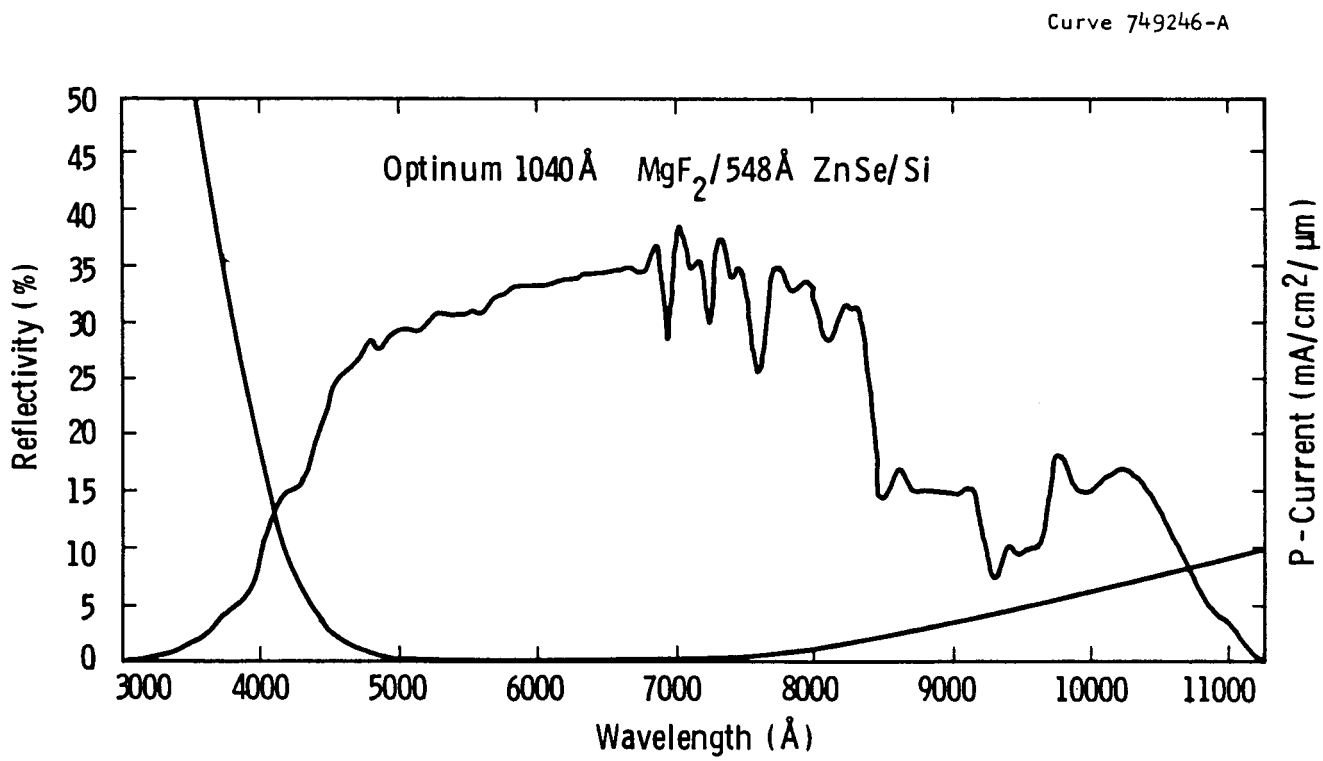

Figure 1. Model calculations showing 51.7% enhancement in short-circuit current density with 548 Å ZnSe + 1040 Å MgF_2 on top of bare silicon.

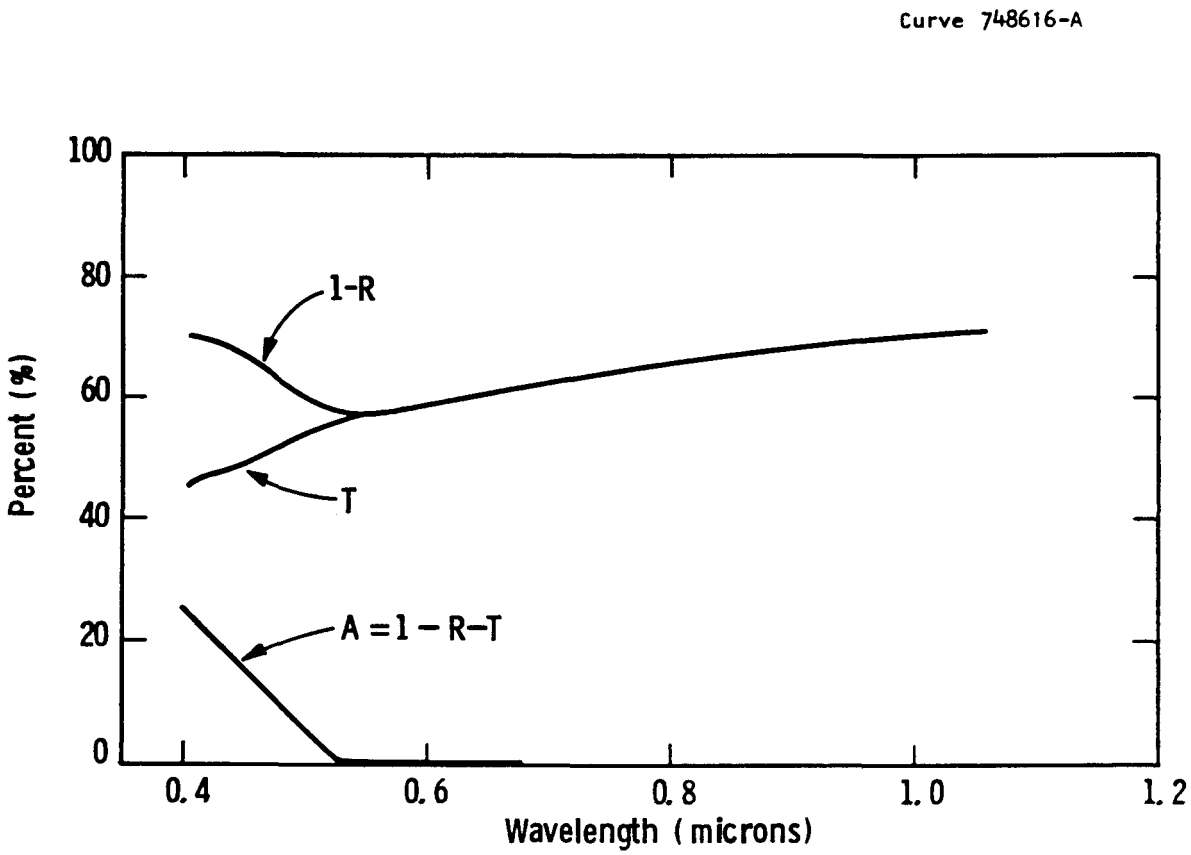

Figure 2. Optical properties of ZnSe films on silicon.

Curve 748617-A

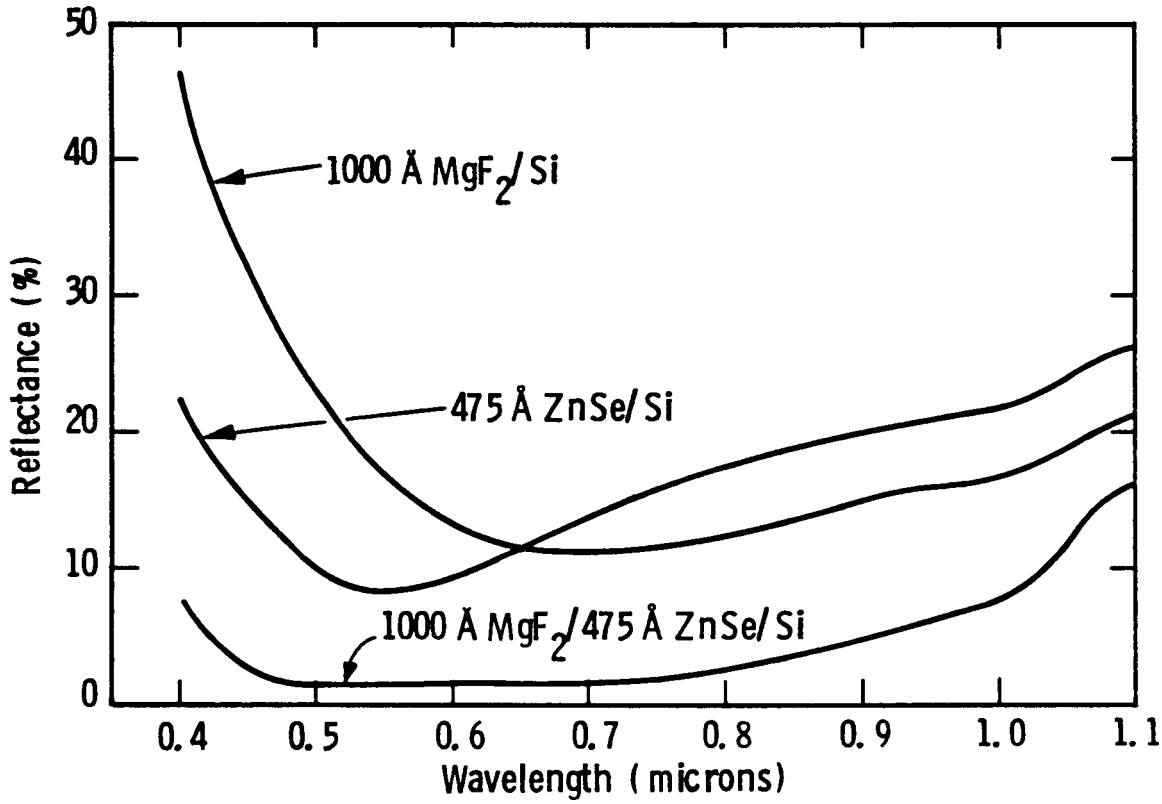

Figure 3. Experimentally determined reflectance curves for a) 1000 Å MgF_2/Si, b) 475 Å ZnSe/Si, and c) 1000 Å MgF_2/475 Å ZnSe/Si.

TABLE 1

Effect Of 550 A° ZnSe + 1040 A° MgF_2 Evaporated Double Layer AR Coating On Unpassivated Cells

Cell ID	Cell Area (cm^2)	Surface Condition	J_{sc} mA/cm^2	V_{oc} mV	FF	η %	Improvement in J_{sc}
HIEFY 19-3.1	1.0	Before AR	23.9	600	0.803	11.5	
		After AR	34.6	609	0.798	16.8	45%
HIEFY 19-2.3	1.0	Before AR	23.2	605	0.797	11.2	
		After AR	34.5	613	0.800	17.0	48%
HIEFY-119-Web 2B-2	1.0	Before AR	22.4	549	0.785	9.7	
		After AR	33.2	565	0.789	14.8	48%
HIEFY 19-Web 86B-3	1.0	Before AR	23.8	569	0.775	10.51	
		After AR	34.2	580	0.769	15.3	44%
		AR + Sinter	35.9	583	0.774	16.2	50%
AESD Web-80 A	19.6	Before AR	21.9	585	0.759	9.7	
		After AR	32.1	593	0.768	14.6	47%

MgF_2. In the best case we have seen as much as 50% improvement in the short-circuit current density. The experimentally observed improvement is smaller than calculated improvements of 51.7%, probably due to the absorption in the ZnSe film. Table 1 shows some variation in the improvement, but the scatter is decreasing with increasing experience in depositing the films.

3.1.2 Dendritic Web Solar Cells with Evaporated ZnSe + MgF_2 Double-Layer AR Coating

Table 2 shows some 16% efficient 4 ohm-cm dendritic web silicon solar cells with evaporated double-layer as coating. These cells were about 10.5% efficient prior to AR coating and, as a result of double-layer AR coating, the J_{sc} increased from 23.8 mA/cm^2 to 35.9 mA/cm^2 and cell efficiency went up to 16.2%. These cells had no oxide passivation or back-surface reflector.

3.2 Development of Aluminum Back-Surface Reflector for High-Efficiency Web Solar Cells

Dendritic web silicon cells are generally thin (5-6 mils) and some long-wavelength photons are therefore not absorbed in the web silicon. Figure 4 shows that about 400 μm thick silicon is needed to absorb all the usable photons in silicon, and 125 μm thick web silicon absorbs only 93% of the usable photons. Therefore, 7% of the unabsorbed photons are lost if an effective back-surface reflector is not used. In any present cell design we use Ti-Pd-Ag back metal, but Ti has a poor reflectivity of about 30% for wavelengths greater than 0.9 μm. Table 3 shows that aluminum has a reflectivity of greater than 90% for long-wavelength photons ($\lambda > 0.9$ μm). Therefore, we decided to use Aℓ-Ti-Pd-Ag as our back metal as opposed to straight Ti-Pd-Ag. The reflected photons by the Aℓ reflector will get one extra pass through the cell and generate more carriers. Figure 5 shows the effect of the Aℓ back-surface reflector on the internal quantum efficiency of web cells. The cells with Aℓ BSR showed a very definite increase in long-

TABLE 2

D175-68

High Efficiency Web Solar Cells With 550 Å ZnSe + 1040 Å MgF_2 Double Layer AR Coating

Cell ID	Cell Area cm^2	J_{sc} mA/cm^2	V_{oc} Volts	FF	η %
86B-1	1.0	35.7	0.583	0.774	16.1
86B-2	1.0	35.9	0.583	0.772	16.2
86B-3	1.0	35.9	0.583	0.774	16.2
86B-4	1.0	35.9	0.581	0.767	16.0

*AM1, 100 mW/cm^2 Illumination
Run # HIEFY 19

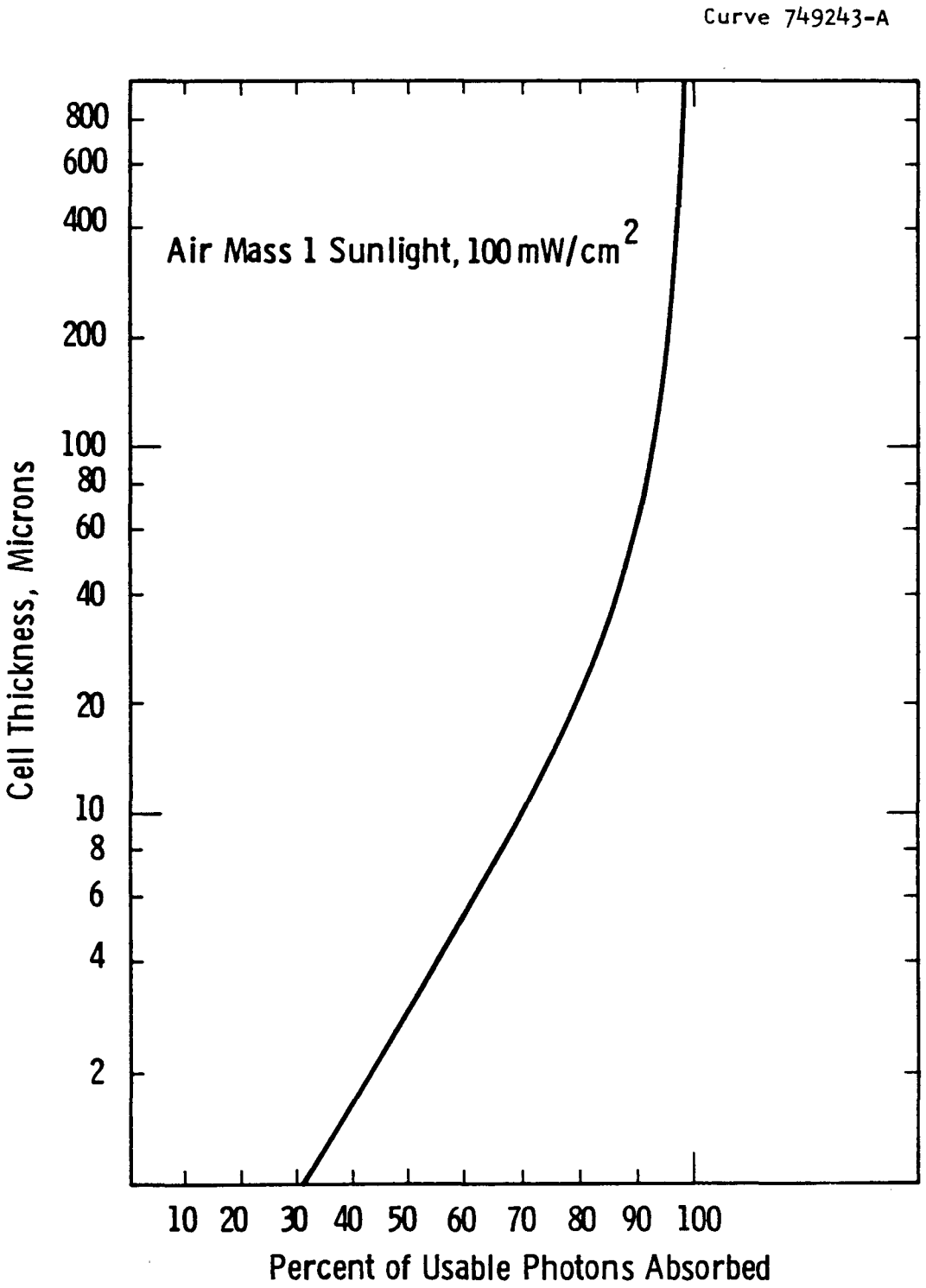

Figure 4. Energy absorption as a function of silicon thickness.

Table 3

Percent Reflectance of Freshly Evaporated Mirror Coatings (Normal-Incidence)

λ(μm)	Aℓ	Ag	Au	Cu
0.220	91.5	28.0	27.5	40.4
0.240	91.9	29.5	31.6	39.0
0.260	92.2	29.2	35.6	35.5
9.280	92.3	25.2	37.8	33.0
0.300	92.3	17.6	37.7	33.6
0.315	92.4	5.5	37.3	35.5
0.320	92.4	8.9	37.1	36.3
0.340	92.5	72.9	36.1	38.5
0.360	92.5	88.2	36.3	41.5
0.380	92.5	92.8	37.8	44.5
0.400	92.4	95.6	38.7	47.5
0.450	92.2	97.1	38.7	55.2
0.500	91.8	97.9	47.7	60.0
0.550	91.5	98.3	81.7	66.9
0.600	91.1	98.6	91.9	93.3
0.650	90.5	98.8	95.5	96.6
0.700	89.7	98.9	97.0	97.5
0.750	88.6	99.1	97.4	97.9
0.800	86.7	99.2	98.0	98.1
0.850	86.7	99.2	98.2	98.3
0.900	89.1	99.3	98.4	98.4
0.950	92.4	99.3	98.5	98.4
1.0	94.0	99.4	98.6	98.5
1.5	97.4	99.4	99.0	98.5
2.0	97.8	99.4	99.1	98.6

Curve 747968-A

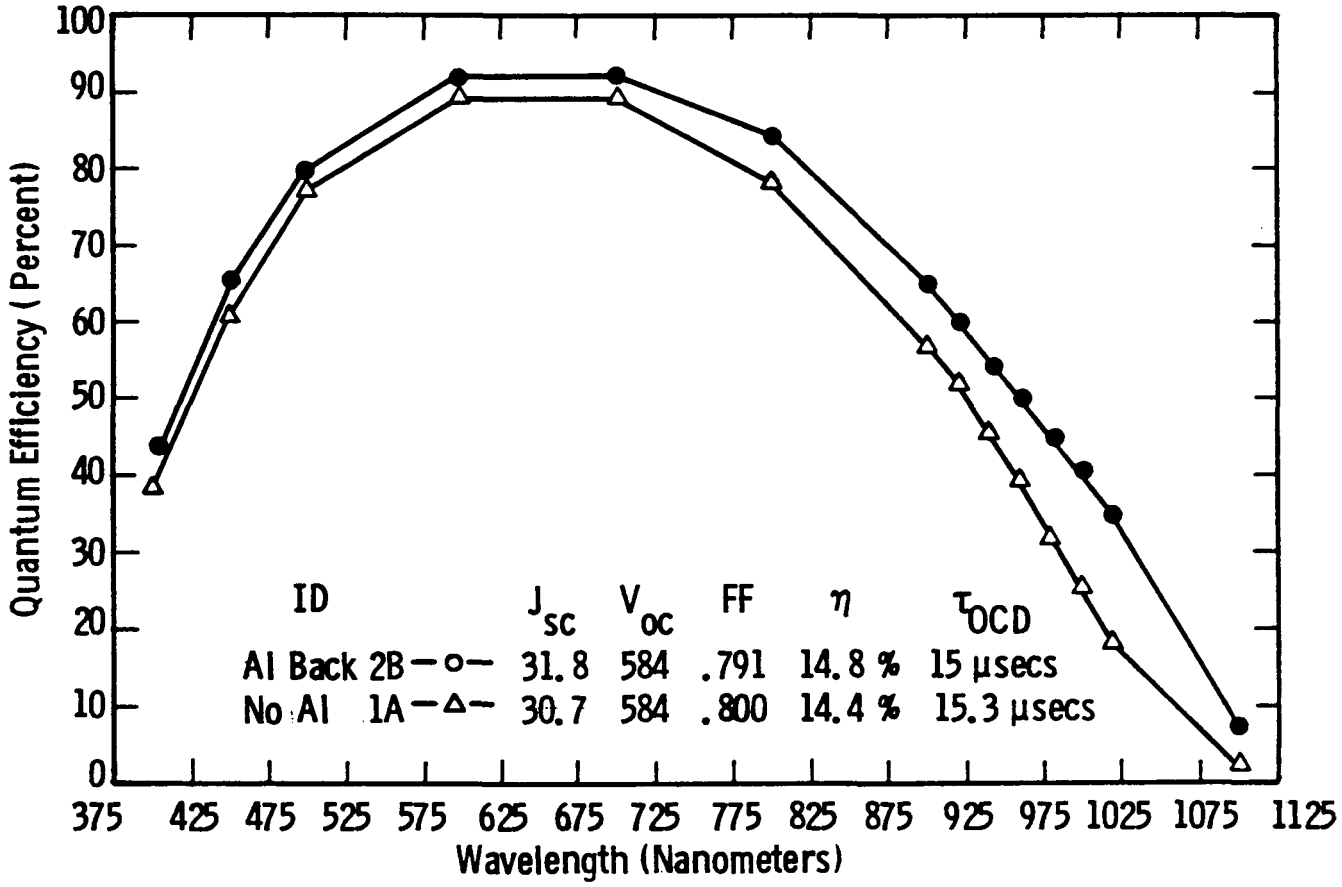

Figure 5. Effect of aluminum back-surface reflector on web cell performance.

wavelength response compared to the one without the Aℓ back metal reflector. Improved long-wavelength response could come either from the higher bulk lifetime or by generation of more carriers in the bulk by the reflected photons. In the latter case bulk lifetime remains unaltered. We performed open-circuit voltage decay lifetime (τ_{OCD}) measurements to make sure that this enhancement is not due to the difference in the bulk lifetime of the two cells. In both cells the τ_{OCD} was ~ 15 μsecs supporting the premise that the enhanced long-wavelength response is primarily due to the generation of more electron-hole pairs by the reflected photons into the cell. The cell data in Figure 5 also show that the primary difference in cell performance comes from the 1 mA/cm^2 increase in the short-circuit current density, which results in about 0.5% absolute increase in cell efficiency. It should be recognized that the absolute improvement in J_{sc} depends on the minority carrier diffusion length in the starting material, and a higher diffusion length would show greater improvement.

3.3 High-Efficiency Web Solar Cells with Oxide Passivation, Double-Layer Antireflective Coating, and Aluminum Back-Surface Reflector

We have made an attempt to combine oxide surface passivation, double-layer antireflective coating, and an aluminum back-surface reflector on web cells. In this experiment we needed a lower resistivity web material (0.37 ohm-cm, crystal ID#4-275-10). Table 4 shows the web cell data from this run. Open-circuit voltages of 600 mV, short-circuit current density of 35 mA/cm^2, and cell efficiencies approaching 17% were achieved. Dark I-V measurements on a 16.9% web cell showed a series resistance of 0.4 ohm-cm, shunt resistance of 1.2 mega-ohms, and reverse saturation current $J_o = 2 \times 10^{-12}$ A/cm^2. Open-circuit voltage decay lifetime was 13 μsecs, which corresponds to a diffusion length of ~ 153 μm for 0.37 ohm-cm silicon ($L = \sqrt{D\tau} = \sqrt{18 \times 13 \times 10^{-6}} \div 153$ μm). The diffusion length measured by the surface photovoltage technique was only 86 μm, probably because the SPV measurement tends to give an erroneous or lower diffusion length when the diffusion length becomes

Table 4

Low-Resistivity (0.37 ohm-cm) High-Efficiency Web Solar Cells With Surface Passivation, Back-Surface Reflector, and Evaporated Double-Layer AR Coating

D175-131

Cell ID	Area cm^2	J_{sc} mA/cm^2	V_{oc} mV	FF	η %
1-1	1.0	35.2	600	0.800	16.9
1-2	1.0	35.2	600	0.800	16.9
1-3	1.0	35.0	598	0.802	16.8
1-4	1.0	34.9	598	0.800	16.7
1-5	1.0	35.2	596	0.793	16.7
1-6	1.0	35.1	596	0.792	16.6

*Run # Hiefy 20, Web #1
*AM1, 100 mW/cm^2 Illumination

comparable or greater than the cell thickness. In addition, SPV measurements were made without white-light bias.

Figure 6 shows the internal quantum efficiency plot for the 16.9% efficient web cell, which looks consistent with the diffusion length of $\leq$ 150 μm. It is difficult to extract a line bulk diffusion length from this plot because the effect of the back-surface reflector has contributed to the increase in long-wavelength response. A plot[2] of $1/\alpha$ V_s x -1, which is used to extract diffusion length from quantum efficiency data, gives a curve (Figure 7) instead of straight line due to the effect of the back-surface reflector.

Figure 8 shows the measured reflectance as a function of wavelength for the 16.9% efficient web cells. Since this cell had 100 Å passivating oxide, the thickness of ZnSe and MgF_2 were adjusted to 398 Å and 1080 Å, respectively, to obtain the best results from AR coating. According to model calculations, 1080 Å MgF_2 + 398 Å ZnSe + 100 Å SiO_2 on top of a bare silicon cell should produce a 51.7% enhancement in short-circuit current density, assuming no absorption in any film. Figure 8 reveals two important features: first, a very low reflectance (less than 2%) in the wavelength range of 0.4 to 0.8 μm due to the double-layer AR coating, and secondly a sharp rise in the reflectance in the wavelength range of 0.9 to 1.1 μm due to the aluminum back-surface reflector. The unabsorbed photons in the wavelength range of 0.9 to 1.1 μm are reflected back into the cell, get one more pass through the cell, and come out through the front surface to give an indication of high reflectance. We see very high reflectance at the long wavelengths because web material is relatively thin (125 μm) compared to the absorption depth of the long-wavelength photons. In silicon, the absorption depth for a wavelength of 1 μm is about 134 μm.

Thus the reflectance curve of Figure 8 indicates that both double-layer AR coating and an aluminum back-surface reflector are very effective in these web cells; their combined effect, therefore, gives a short-circuit current density of 35 mA/cm^2. Table 5 shows that without

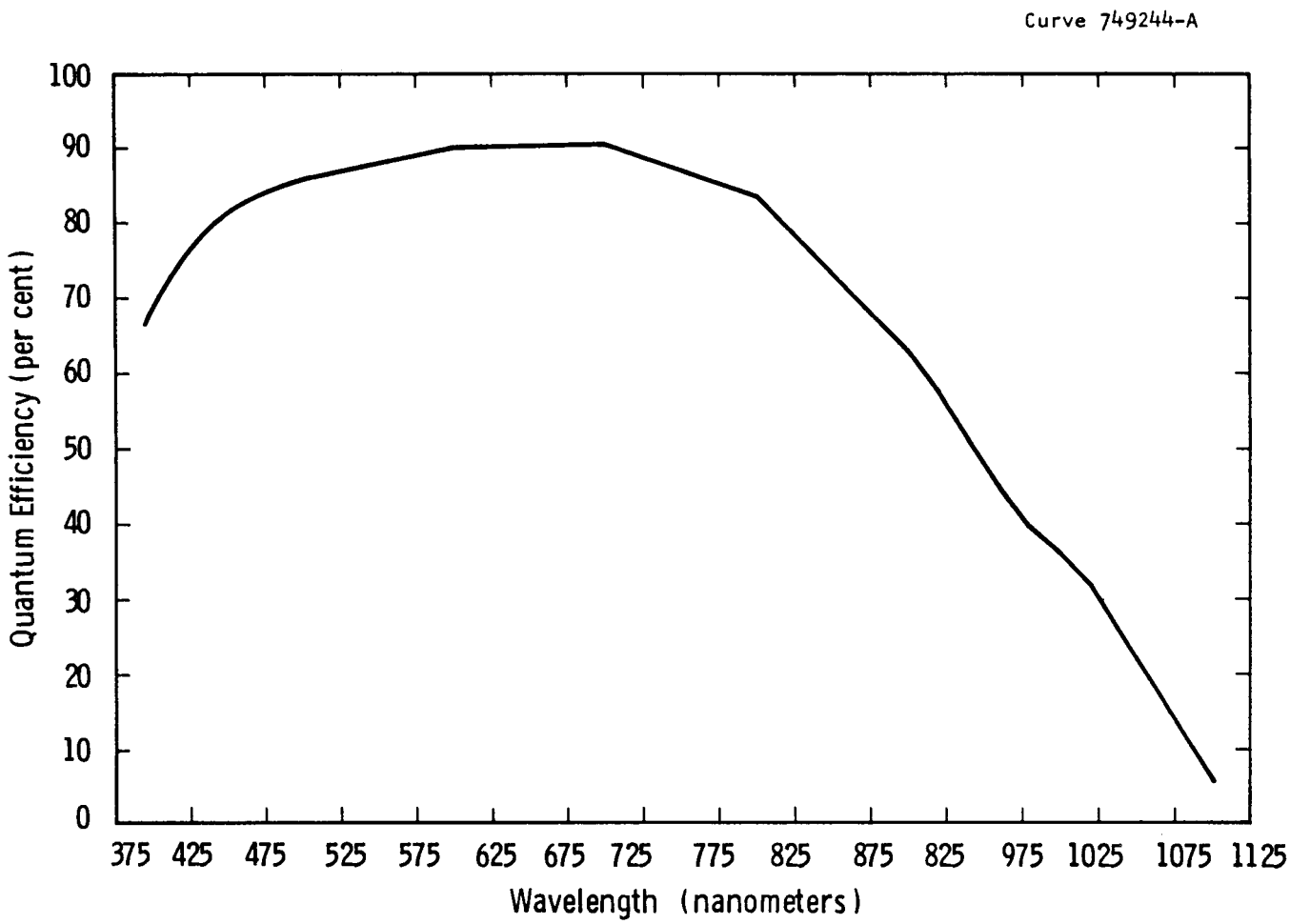

Figure 6. Internal quantum efficiency versus wavelength plot for 16.9% efficient web solar cell with oxide passivation, evaporated double-layer AR coating, and aluminum back-surface reflector (Hiefy 20, web 1-4)

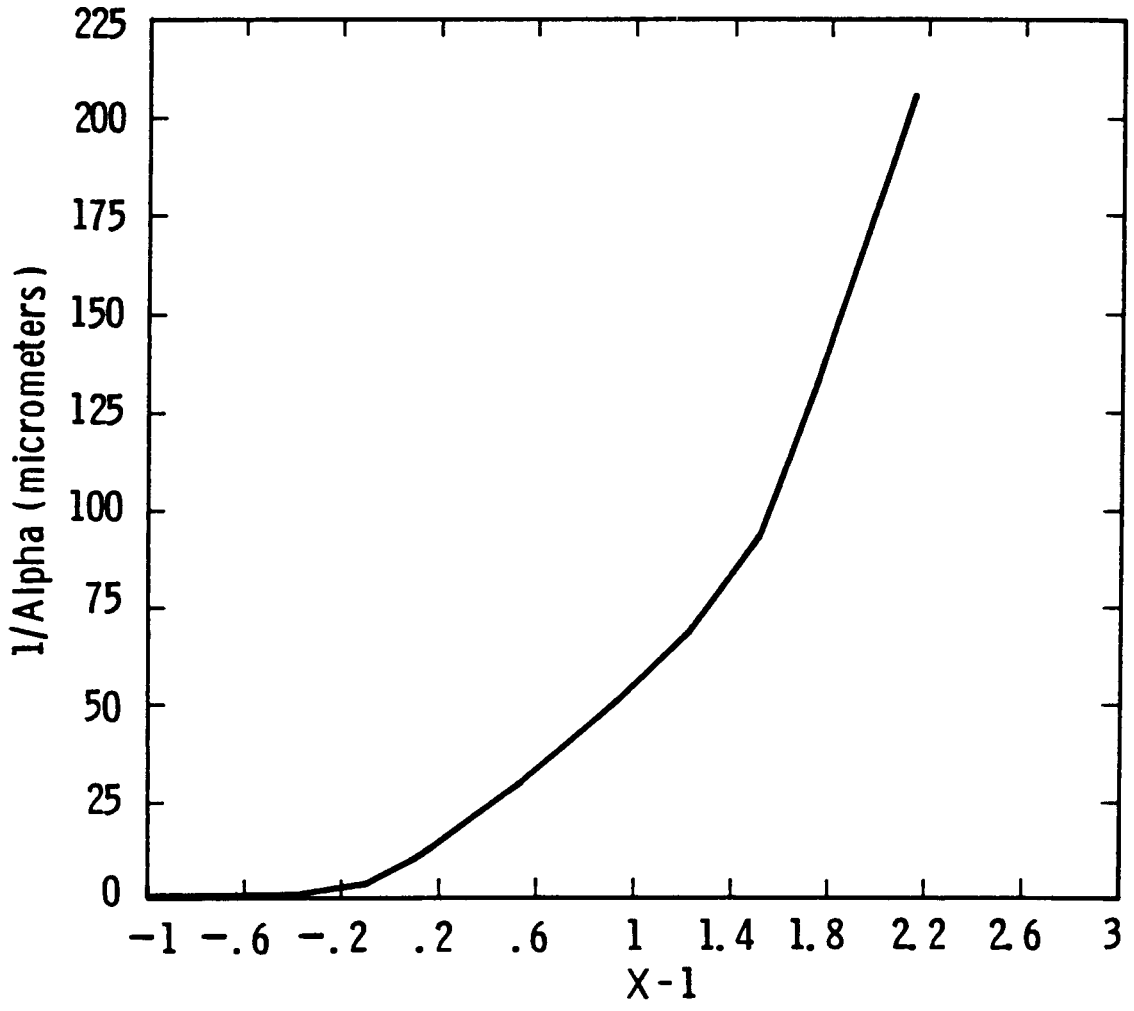

Figure 7. Plot of x-1 versus 1/α, which is used obtain diffusion length, for 16.9% efficient web solar cell. Due to back-surface reflector effect, a curvature is observed in the plot instead of a straight line.

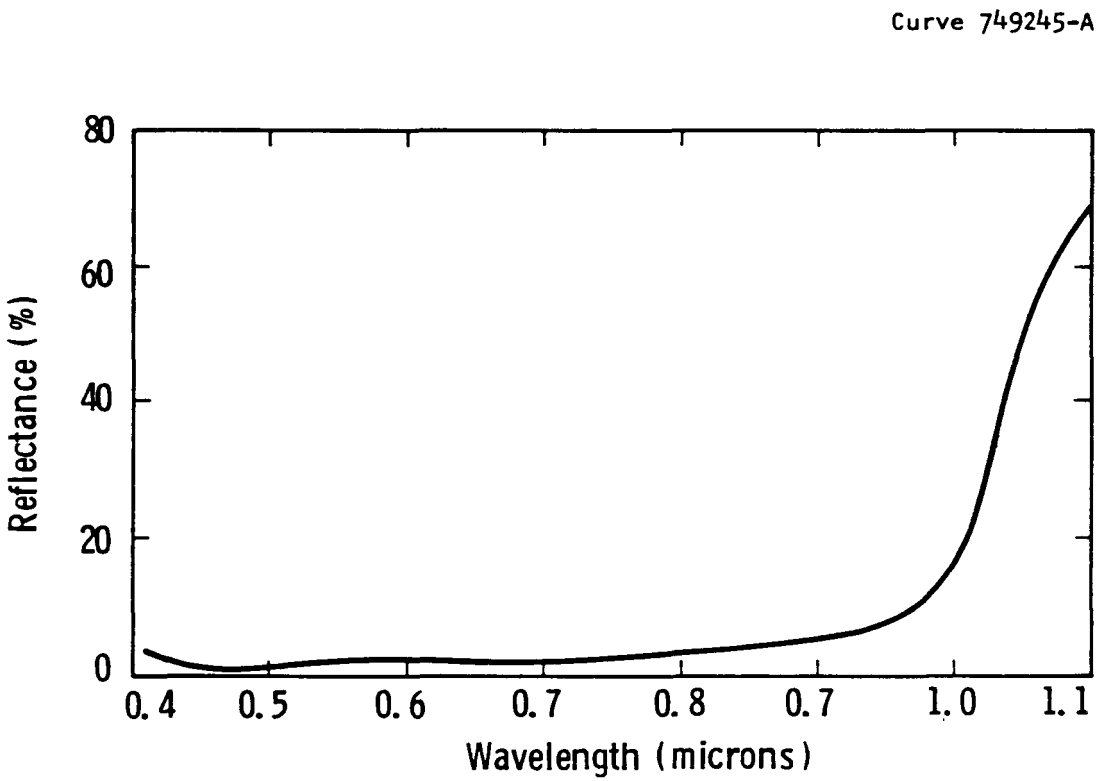

Figure 8. Reflectance as a function of wavelength for 16.9% efficient web cell with oxide passivation, evaporated ZnSe + MgF_2 double-layer antireflective coating, and aluminum back-surface reflector.

Table 5

Baseline Web Solar Cells on 0.37 ohm-cm Web (Crystal #4-275) Without Antireflective Coating, Back-Surface Reflector, and Oxide Passivation

Cell ID	J_{sc} mA/cm^2	V_{oc} mV	FF	Efficiency %
6-1-2	21.3	579	.790	9.7
6-2-6	21.6	575	.803	10.0
6-3-6	22.1	574	.778	9.9

Hiefy 20, Qual.
Crystal #6
AM1, 100 mW/cm^2 illumination

oxide passivation, double-layer AR coating, and the back-surface reflector, the short-circuit current density is only about 22 mA/cm^2 and the cell efficiency is ~ 10%. A combination of oxide passivation, double-layer AR coating, and Aℓ back-surface reflector provides about 59% improvement in J_{sc} and 69% increase in cell efficiency. It should be recognized that the amount of improvement in J_{sc} or cell efficiency is a strong function of material quality or diffusion length in the material.

4. PROGRAM STATUS

4.1 Present Status

The current milestone chart for this program is shown in Table 6. During this three-month period we have:

- Developed evaporated ZnSe + MgF_2 double-layer AR coating for web cells.
- Developed a process sequence for incorporating an aluminum back-surface reflector on web cells.
- Fabricated 16.2% efficient solar cells on 4 ohm-cm web crystals.
- Fabricated 16.9% efficient web solar cells with oxide passivation, double-layer AR coating, and an Aℓ back-surface reflector on 0.37 ohm-cm web crystal.

4.2 Future Activity

Plans are to conduct more LBIC and EBIC measurements on web cells to understand the role of twin plane activity in web. Heat-treatment studies will be continued to improve the diffusion length in web, and cells will be fabricated on low-resistivity dendritic web crystals.

Table 6

MILESTONE CHART

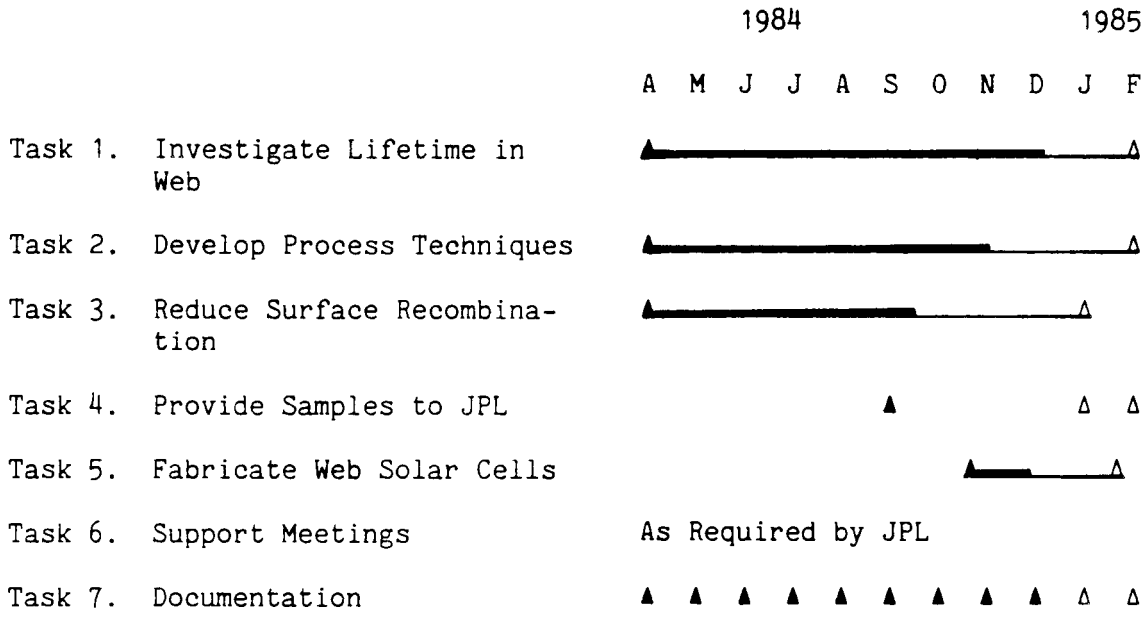

5. REFERENCES

1. M. Wolf. "Designing Practical Silicon Solar Cells Approaching the Limit Conversion Efficiency," Proc. 14th IEEE Photovoltaic Specialists Conf. p. 563 (1980).

2. A. Rohatgi and P. Rai-Choudhury, "Research on the Basic Understanding of High Efficiency in Silicon Solar Cells," Annual Report, SERI Contract No. XB-3-02090-4, March 1984.

6. ACKNOWLEDGMENTS

The authors would like to thank J. B. McNally, F. S. Youngk, and G. J. Machiko for cell fabrication; R. A. Hoffman and B. Blankenship for evaporated double-layer AR coating; S. Karako for surface photovoltage measurements and assisting with the model calculations; and G. S. Law for reading and preparing the manuscript.